Processing and Application of Ceramics 14 [3] (2020) 203–209
https://doi.org/10.2298/PAC2003203V

Influence of temperature and oxygen pressure on the stability of barium or strontium doped neodymium manganites

Larisa Vedmid'[1,2,*], Olga Fedorova[1], Valentina Balakireva[3], Vladimir Balakirev[1]

[1]*Institute of Metallurgy, Ural Branch, Russian Academy of Sciences, Postal Code 620016, Amundsen St., 101, Yekaterinburg, Russia*
[2]*Ural Federal University, Postal Code 620002, Mira St., 19, Yekaterinburg, Russia*
[3]*Institute of High-Temperature Electrochemistry, Ural Branch, Russian Academy of Sciences, Postal Code 620137, Academicheskaya St., 20, Yekaterinburg, Russia*

Received 26 March 2020; Received in revised form 13 April 2020; Received in revised form 16 June 2020; Accepted 7 July 2020

Abstract

In this work neodymium manganites, $Nd_{1-x}A_xMnO_{3\pm\delta}$, doped with Ba or Sr (where x = 0.15 and 0.25) were obtained by ceramic technology at 1250 °C. In order to obtain materials with stable thermal and electrical properties, their structure and physicochemical properties were studied depending on the dopant type and its concentration. It was established that the manganites doped with strontium (for x = 0.15 and 0.25) and barium (for x = 0.15) have the Jahn-Teller distortion of the structure, but it was not observed for the sample $Nd_{0.75}A_{0.25}MnO_{3\pm\delta}$. The sequence of phase transformations was studied under conditions of reduced oxygen pressure in gaseous phase using thermal analysis in combination with XRD. The influence of temperature and oxygen pressure on the stability limit of the manganites was investigated. The studied manganites remain stable in the range of partial oxygen pressures P_{O_2} from 0.21 to 10^{-14} atm at 800 °C. An increasing in the dopant concentration leads to the increase of manganite electrical conductivity without decreasing the thermal stability limit.

Keywords: *manganite perovskites, SOFC, structural characterization, superconductivity, thermal properties*

I. Introduction

The practical importance of $Ln_{1-x}A_xMnO_{3\pm\delta}$ manganites (Ln^{3+} = lanthanide cation, A^{2+} = alkaline earth metal) is associated with the prospect of using them as cathode materials for solid oxide fuel cells (SOFC) [1–4]. Another factor that attracts an attention to these materials is the variety of its physicochemical properties [5–10]. The degree of correlation between the electric and magnetic properties may depend on the concentration and type of dopant. It is explained by the double exchange mechanism between polyvalent manganese ions $Mn^{3+} \leftrightarrow Mn^{4+}$ [11–16]. The difference between ionic radii of the lanthanide and the dopant affects to formation of the Jahn-Teller distortion in these manganites [17]. Variation of dopant concentration in wide range affects the magnetic, structural, charge and orbital ordering [18–20]. At some ratios of Mn^{3+}/Mn^{4+} there are various types of orders and superstructures in these compounds [5, 21]. For a reasonable choice of an optimal composition of the compounds for practical use, information about physicochemical characteristics of the corresponding systems and their phases are needed. Information about the oxygen content in various compositions of $Ln_{1-x}A_xMnO_3$ perovskites and its most important properties, such as electrical conductivity and thermal stability, and their dependence on external parameters are scarce.

The purpose of this work is to establish relationship between the chemical composition and physicochemical properties of oxides at different temperatures and oxygen partial pressures.

*Corresponding author: tel: +7 343 2679186,
e-mail: *elarisa100@mail.ru*

II. Materials and methods

The synthesis of $Nd_{1-x}A_xMnO_3$ compounds (where x = 0.15 and 0.25 and A = Ba, Sr) was carried out using ceramic technology from Nd_2O_3 (Merck Aldrich, 99.9%), Mn_2O_3 (Sigma Aldrich, 99.9%) and carbonates ($BaCO_3$ or $SrCO_3$) qualified as "high purity". Required amount of initial components were carefully mixed, pressed at a pressure of 100 MPa in pellet and finally thermally treated at 1250 °C for 70 h in air, followed by cooling together with the furnace.

The phase composition of the initial samples and their dissociation products was studied using XRD-7000 diffractometer (Shimadzu), with CuK_α radiation in an angle range of 20–70° by increment of 0.03° and exposure time of 2 s.

The thermal stability of the $Nd_{1-x}A_xMnO_3$ compounds (where x = 0.15 and 0.25 and A = Ba, Sr) under conditions of low oxygen partial pressure was studied by the static method using a vacuum circulation unit [22]. The used experimental installation ensured the temperature accuracy of ±2 °C, the partial oxygen pressure $\log P_{O_2}$ of ±0.1 and the quantity of oxygen removed from the initial sample of ±1.0 at.%. The samples were preliminarily weighed to determine their absolute oxygen content, then heated in a vacuum circulation unit to 800 °C and kept at this temperature for 70 h in an atmosphere with partial oxygen pressure $P_{O_2} = 10^{-25}$ atm. This ensured their reduction to stable oxides. The reduction completeness was confirmed by X-ray diffraction analysis (XRD) of the heat-strengthened products of this process. The applied method allows us to determine the absolute amount of oxygen in the original sample. It was assumed that the mass loss after reduction refers only to non-stoichiometric oxygen of the initial product (the assumption is made that there is no significant oxygen non-stoichiometry of the reduction products in our experiment) [22].

The evolution of phase equilibria in the compounds was studied using the STA 449 F3 Jupiter (Netzsch) synchronous thermal analysis instrument, fitted with an attachment for creating gas atmospheres with varying oxygen pressures [23]. The experiment was carried out in the linear heating mode from room temperature to 1200 °C and at rate of 10 °C/min. Pt-Rh alloy crucibles with cover plate were used as a container. The temperature measurement error was no more than ±1.5 °C.

Electrical conductivity was measured by a direct current automated four-probe method using samples in the form of bars 4×4×4 mm with platinum electrodes. Applied electrodes were stained with platinum paste and baked at 1000 °C (1 h). Partial oxygen pressures were created using an electrochemical pump with an automatic regulator. Pressure control was carried out by using an electrochemical sensor which was made from solid electrolyte ceramics with the composition ZrO_2 + Y_2O_3, with platinum electrodes. The reference gas was air. The dependence of electrical conductivity on the partial pressure of oxygen was studied at 800 °C and P_{H_2O} = 3.6 kPa. After reaching the specified partial oxygen pressure, the system was maintained to a constant value of electrical conductivity. The electrical conductivity was considered to be at equilibrium if it was constant during 60 min.

III. Results and discussion

The synthesized homogeneous compounds according to X-ray phase analysis (Fig. 1) have a perovskite structure with orthorhombic distortions (space group *Pbnm*) [13,15,17,24,25]. All samples except the $Nd_{0.75}Ba_{0.25}MnO_3$ have unit cell parameters corresponding to the orbitally ordered *O'* phase at room temperature, i.e. relation $c/\sqrt{2} < a < b$ is valid (Table 1). The sample with the replacement of neodymium by barium at x = 0.25, has parameters similar to a pseudocubic lattice ($a \approx b \approx c/\sqrt{2}$). This fact is explained by the replacement of trivalent neodymium ions with divalent barium ions, which at higher concentration (x = 0.25) leads to the part of Mn^{3+} transforming to Mn^{4+} ions. Electroneutrality condition leads to the unit cell contraction [26] and removing of the Jahn-Teller distortion [17].

Oxygen non-stoichiometry of the obtained compounds was determined as a result of their reduction to stable oxides using a vacuum circulation unit and presented in Table 1. It was assumed that $Nd_{1-x}Ba_xMnO_{3\pm\delta}$ decomposed to: BaO, Nd_2O_3, MnO and O_2, whereas $Nd_{1-x}Sr_xMnO_{3\pm\delta}$ decomposed to: Sr_2MnO_4, Nd_2O_3, MnO and O_2.

The thermal stability of the $Nd_{1-x}A_xMnO_{3+\delta}$ samples was studied using the linear heating regime from room temperature to 1200 °C in gas atmospheres with different oxygen partial pressures. The sample mass increase is fixed after heat treatment in air at partial pressure of oxygen P_{O_2} = 0.21 atm (Fig. 2). While concentration of

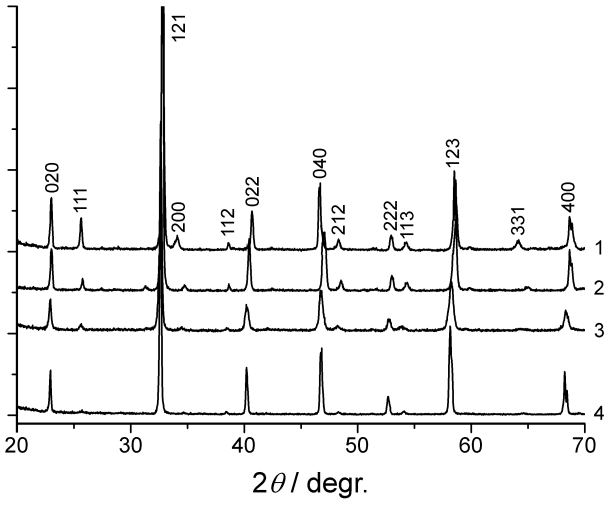

Figure 1. X-ray diffraction patterns of the synthesized samples: $Nd_{0.85}Sr_{0.15}MnO_3$ (1), $Nd_{0.75}Sr_{0.25}MnO_3$ (2), $Nd_{0.85}Ba_{0.15}MnO_3$ (3) and $Nd_{0.75}Ba_{0.25}MnO_3$ (4)

Table 1. Oxygen non-stoichiometry and unit cell parameters of $Nd_{1-x}A_xMnO_{3+\delta}$ samples (where x = 0.15 and 0.25 and A = Ba, Sr)

Compound	a [Å]	b [Å]	c [Å]	δ (at 293 K)
$Nd_{0.85}Ba_{0.15}MnO_{3+\delta}$	5.4627(4)	5.5012(5)	7.7616(6)	0.04(1)
$Nd_{0.75}Ba_{0.25}MnO_{3+\delta}$	5.5040(2)	5.5071(6)	7.7947(5)	0.02(1)
$Nd_{0.85}Sr_{0.15}MnO_{3+\delta}$	5.4373(3)	5.5701(6)	7.6282(6)	0.01(1)
$Nd_{0.75}Sr_{0.25}MnO_{3+\delta}$	5.4676(3)	5.4872(4)	7.7460(8)	0.01(1)

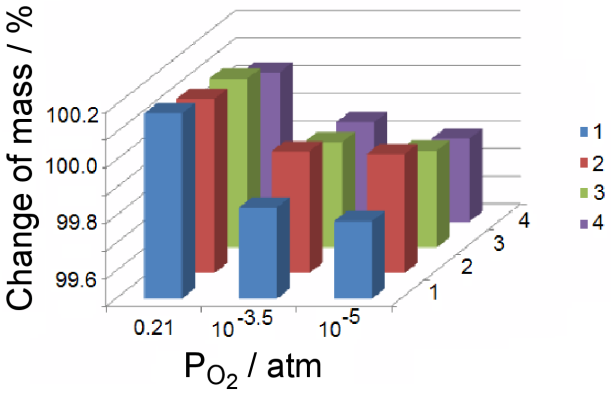

Figure 2. Change of mass under heating to 1200 °C in gaseous phases with different partial pressure of oxygen for the samples: $Nd_{0.85}Sr_{0.15}MnO_3$ (1), $Nd_{0.75}Sr_{0.25}MnO_3$ (2), $Nd_{0.85}Ba_{0.15}MnO_3$ (3) and $Nd_{0.75}Ba_{0.25}MnO_3$ (4)

dopants increases, decline of weight gain is due to their oxidation.

Generally, mass decrease tendency occurs for all samples due to the oxygen content decrease; this in turn happens because oxygen pressure decreases in the gaseous phase. An increase of the dopant fraction is accompanied by the less active mass loss. It should be noted that the barium content rising in oxides reduces the amount of oxygen lost during heating. The effect of strontium concentration in this process is less noticeable.

Endothermic effects were observed by differential scanning calorimetry at T = 230–320 °C for the $Nd_{0.85}A_{0.15}MnO_{3\pm\delta}$ (where A = Ba, Sr) and $Nd_{0.75}Sr_{0.25}MnO_{3\pm\delta}$ samples if heated both in air (Fig. 3a) and under reduced oxygen pressure (Fig. 3b). Destruction of the Jahn-Teller ordering and the formation of the orbitally disordered O phase occurs in this temperature range. The Jahn-Teller transition is fixed at $T \sim 300$ °C for all samples except for the sample with barium content x = 0.25. The absence of the Jahn-Teller transition in this sample is due to the higher barium concentration, i.e. $x > 0.18$ [17]. Such concentration leads to the increase of Mn^{4+} ions content due to the replacement of Nd^{3+} ions by Ba^{2+} ions, changes in the lengths of Mn–O bonds and removal of the Jahn-Teller distortion. This is caused by a size factor. The ionic radius of barium r_{Ba^6} = 1.35 Å is greater than the ionic radius of strontium r_{Sr^6} = 1.20 Å and significantly greater than the ionic radius of neodymium r_{Nd^6} = 0.98 Å [26].

The increase of dopant concentration leads to slight decrease of the Jahn-Teller transition temperature. Subsequent heating in air leads to oxidation of all samples and transition to pseudocubic structure at $T \sim$ 1000 °C. Similar processes are observed at pressures $P_{O_2} = 10^{-3.5}$ atm and $10^{-5.0}$ atm. However, at reduced oxygen pressure the transition temperature to pseudocubic structure is shifted toward lower temperatures compared with air (Fig. 3b).

Two methods are used for the estimation of the phase equilibria sequence and thermal stability of the studied oxides when the oxygen pressure changes in gaseous phase. The first is static if a vacuum circulation system is used. The other is dynamic if a thermal analysis device fitted with an isobaric attachment is used. The static method help us trace the sequence of phase equilibria if we remove fixed portions of oxygen from $Nd_{1-x}A_xMnO_3$ (where x = 0.15 and 0.25 and A = Ba, Sr) oxides; meanwhile the system have to turn into equilibrium between the gas and solid phases. Stepped decrease of the oxygen pressure in the gas phase at constant temperature (T = 830 °C) leads to the oxygen non-stoichiometry

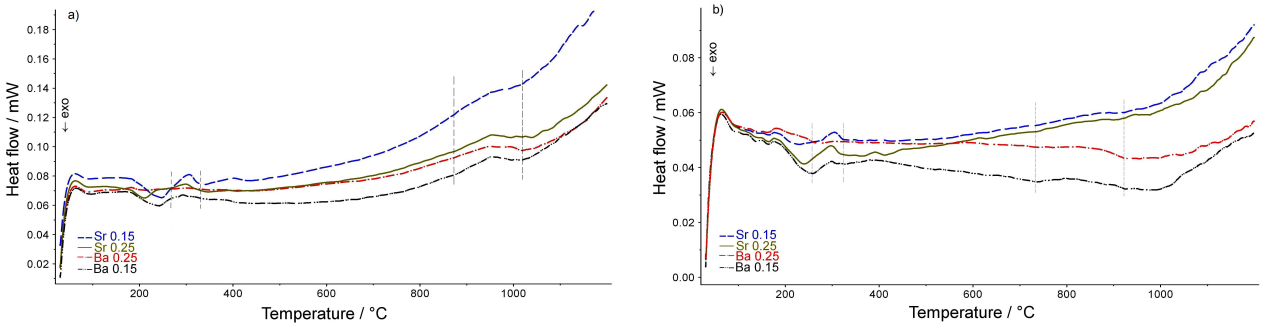

Figure 3. DSC curves for $Nd_{1-x}A_xMnO_3$ samples (where x = 0.15 and 0.25 and A = Ba, Sr) at heating in gaseous phases with partial pressure of oxygen: a) P_{O_2} = 0.21 atm, b) $P_{O_2} = 10^{-5}$ atm

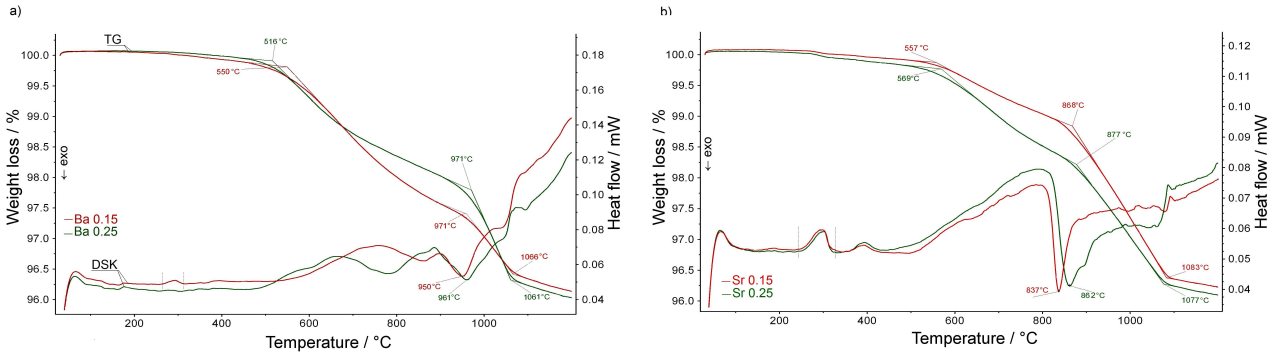

Figure 4. TG and DSC curves of samples: a) $Nd_{1-x}Ba_xMnO_3$ and b) $Nd_{1-x}Sr_xMnO_3$ (where x = 0.15 and 0.25) when heated in gaseous phase with an oxygen pressure $P_{O_2} = 10^{-22.5}$ atm

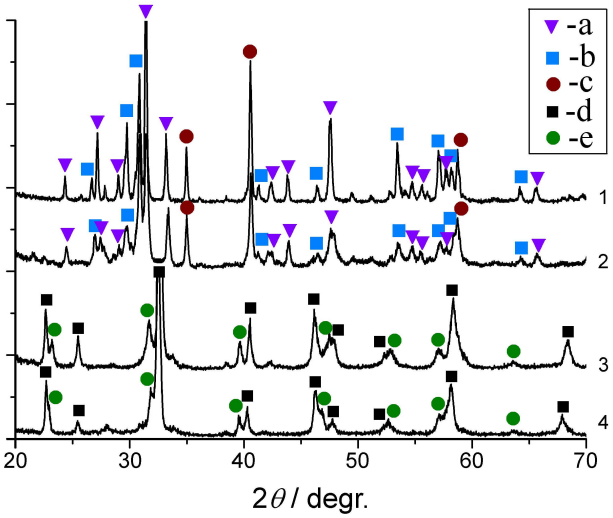

Figure 5. X-ray diffraction patterns of samples after heated in gaseous phase with an oxygen pressure $P_{O_2} = 10^{-22.5}$ atm after the first stage of dissociation: $Nd_{0.85}Sr_{0.15}MnO_3$ (1), $Nd_{0.75}Sr_{0.25}MnO_3$ (2), $Nd_{0.85}Ba_{0.15}MnO_3$ (3) and $Nd_{0.75}Ba_{0.25}MnO_3$ (4) (a - $Sr_{2-y}Nd_yMnO_4$, b - Nd_2O_3, c - MnO, d - $Nd_{0.7}Ba_{0.3}MnO_3$, e - $NdMnO_3$)

change in the oxides in the first stage, and then it leads to dissociation. At the first stage $Nd_{1-x}Ba_xMnO_3$ decomposed to $Nd_{0.7}Ba_{0.3}MnO_3$, $NdMnO_3$ and O_2. At the second stage BaO, Nd_2O_3, MnO and O_2 are formed [25]. $Nd_{1-x}Sr_xMnO_3$ decomposed sequentially at the beginning to $Sr_{2-y}Nd_yMnO_4$, Nd_2O_3, MnO and O_2, then to Sr_2MnO_4, Nd_2O_3, MnO and O_2 [27]. Manganite dissociation to products occurs in the first stage at pressure $P_{O_2} = 10^{-14}$ atm. Dissociation in the second stage occurs with a decrease in pressure of $P_{O_2} \leq 10^{-21}$ atm.

The sequence of phase transformations in manganites is confirmed by the results of studies using the dynamic method. The linear heating of doped neodymium manganites under isobaric conditions (partial pressure of oxygen in gaseous phase $P_{O_2} = 10^{-22.5}$ atm) leads to their sequential two-stage decomposition. In the 230–320 °C temperature range endothermic effects are observed on the DSC curves (Figs. 4a and 4b) for all samples except the $Nd_{0.75}Ba_{0.25}MnO_3$. They are accompanied by slight mass loss and indicated as the Jahn-Teller transition. The absence of the Jahn-Teller transition in the DSC curve of the neodymium manganite with x = 0.25 of barium is associated with the dopant presence in higher concentration, leading to the removal of the Jahn-Teller distortion. Following temperature increase leads to the formation of stoichiometric oxides in oxygen content, then the change in the mass of the samples is determined by the degree of its dissociation. Heating above 800 °C leads to the formation of complex metastable oxides (the first stage of dissociation). It is revealed by the exothermic effects on the DSC curves with peaks at 950 and 961 °C for the samples with barium, and 837 and 862 °C for the samples with strontium, respectively. Figure 5 shows the XRD data for the products of the first stage of manganite dissociation (T = 1000 °C).

The dissociation of the prepared oxides in the temperature range of 1060–1090 °C is completed, confirmed by the formation of Nd_2O_3, MnO and BaO or Sr_2MnO_4 phases (the second stage of dissociation). Decomposition temperatures are indicated on the TG curves. This

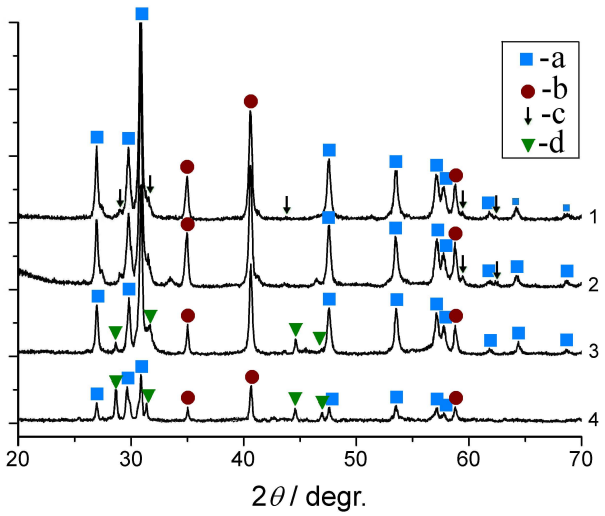

Figure 6. X-ray diffraction patterns of samples after heating in gaseous phase with an oxygen pressure $P_{O_2} = 10^{-22.5}$ atm after the second stage of dissociation: $Nd_{0.85}Sr_{0.15}MnO_3$ (1), $Nd_{0.75}Sr_{0.25}MnO_3$ (2), $Nd_{0.85}Ba_{0.15}MnO_3$ (3) and $Nd_{0.75}Ba_{0.25}MnO_3$ (4) (a - Nd_2O_3, b - MnO, c - Sr_2MnO_4, d - BaO)

is confirmed by the X-ray data of the experiment products (Fig. 6). Some mass loss of the samples, which is visualized under further heating to 1200 °C, is due to the change in the non-stoichiometry of dissociation products: oxides BaO and Sr_2MnO_4. Barium concentration increasing leads to temperature decrease of the manganites dissociation beginning. The increase of strontium dopant concentration shifts the dissociation temperature beginning toward higher temperature, but practically does not change the dissociation temperature finish at our experimental conditions.

The thermal sustainability of $Nd_{1-x}A_xMnO_3$ compounds (where $x = 0.15$, 0.25 and A = Ba, Sr) at reduced oxygen pressure in the temperature range 700–800 °C was estimated by the static method. The equilibrium thermal dissociation of crystalline substances at specific temperature corresponds to the certain value of equilibrium dissociation pressure [28]. The temperature dependences of the equilibrium oxygen partial pressure during the dissociation of $Nd_{1-x}A_xMnO_3$ compounds (where x = 0, 0.15, 0.25 and A = Ba, Sr) to stable oxides were obtained and shown in Fig. 7 by lines a, b, c, d and e.

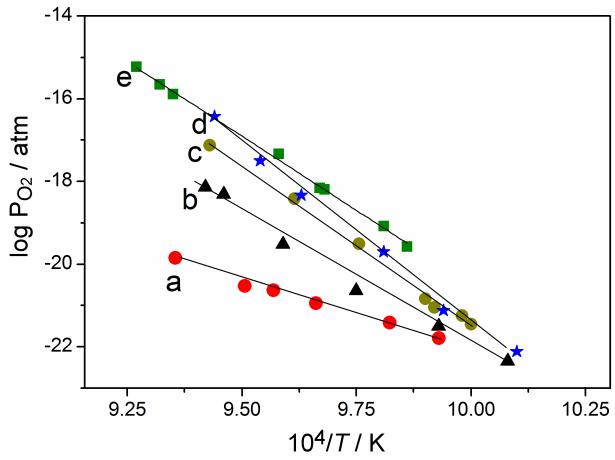

Figure 7. Equilibrium partial oxygen pressure temperature dependences of the dissociation reactions: $Nd_{0.75}Ba_{0.25}MnO_3$ (a) $Nd_{0.85}Ba_{0.15}MnO_3$ (b) $Nd_{0.75}Sr_{0.25}MnO_3$ (c) $Nd_{0.85}Sr_{0.15}MnO_3$ (d) and $NdMnO_3$ (e) [29]

The Gibbs free energy changes for the compounds dissociation reactions are represented by expressions (1–4). For $Nd_{0.85}Ba_{0.15}MnO_3$ it is:

$$\Delta G_T^\circ = 357.42 - 0.2363T \pm 3.37\,\text{kJ/mol} \quad (1)$$

for $Nd_{0.85}Sr_{0.15}MnO_3$ it is:

$$\Delta G_T^\circ = 359.15 - 0.2715T \pm 2.6\,\text{kJ/mol} \quad (2)$$

for $Nd_{0.75}Ba_{0.25}MnO_3$ it is:

$$\Delta G_T^\circ = 219.84 - 0.0703T \pm 0.52\,\text{kJ/mol} \quad (3)$$

for $Nd_{0.75}Sr_{0.25}MnO_3$ it is:

$$\Delta G_T^\circ = 281.22 - 0.204T \pm 0.36\,\text{kJ/mol} \quad (4)$$

The Gibbs free energy changes of the undoped neodymium manganite ($NdMnO_3$) are calculated according to following equation [29]:

$$\Delta G_T^\circ = 316.02 - 0.219T \pm 1.66\,\text{kJ/mol} \quad (5)$$

Replaced part of neodymium by barium or strontium for concentration corresponding to $x = 0.15$ slightly increases the standard enthalpy and entropy values changes of the $Nd_{0.85}A_{0.15}MnO_{3\pm\delta}$ (A = Ba, Sr) compounds dissociation reactions. The opposite trend is observed for dopant concentration of $x = 0.25$. The standard enthalpy and entropy changes of the compounds formation from elements were calculated (Table 2) using the obtained data and the thermodynamic functions changes values for the simple oxides formation [30].

The dopant concentration increase has significant effect on the entropy of compounds formation reactions from elements according to Table 2. Thus, decreasing of thermodynamic functions values in the Ba-containing neodymium manganite is due to the concentration of the dopant at which the compound has an orbitally disordered structure. Accordingly, less energy must be spent on its formation and/or dissociation than on the undoped neodymium manganite having an orbitally ordered orthorhombic structure. Doping by strontium at the same concentration ($x = 0.25$) does not remove the Jahn-Teller distortions, but introduces some structural distortions, which also affects the thermodynamic characteristics.

The electrical conductivity of the studied manganites was considered under isothermal conditions at T = 800 °C and changes in the oxygen pressure from P_{O_2} of $10^{-14.5}$ to 0.21 atm in gaseous phase. The choice of temperature and range of partial oxygen pressures is explained by the results of above experiments on the thermal stability of samples obtained by the static method.

Table 2. Standard enthalpy and entropy changes of the compounds formation from elements

Compound	ΔG_T° [kJ/mol] $= -\Delta H_T^\circ + \Delta S_T^\circ \cdot T$/K	
	ΔH_T°	ΔS_T°
$Nd_{0.85}Ba_{0.15}MnO_3$	1595.04 ± 4.67	0.388 ± 0.003
$Nd_{0.85}Sr_{0.15}MnO_3$	1649.98 ± 3.96	0.440 ± 0.002
$Nd_{0.75}Ba_{0.25}MnO_3$	1422.68 ± 1.08	0.222 ± 0.001
$Nd_{0.75}Sr_{0.25}MnO_3$	1572.75 ± 1.63	0.383 ± 0.001
$NdMnO_3$ [29]	1605.81 ± 1.16	0.371 ± 0.001

Table 3. Conductivity values of $Nd_{1-x}A_xMnO_3$ samples (where x = 0.15, 0.25 and A = Sr, Ba) in air and at partial oxygen pressure $P_{O_2} = 10^{-14}$ atm

σ [S/cm]	$Nd_{0.85}Sr_{0.15}MnO_3$	$Nd_{0.75}Sr_{0.25}MnO_3$	$Nd_{0.85}Ba_{0.15}MnO_3$	$Nd_{0.75}Ba_{0.25}MnO_3$
P_{O_2} = 0.21 atm	72.2(1)	131.9(1)	92.2(1)	117.5(1)
$P_{O_2} = 10^{-14}$ atm	66.7(2)	125.6(2)	84.9(2)	108.5(2)

Table 4. Conductivity values of $Nd_{1-x}Sr_xMnO_3$ samples (where x = 0.15, 0.25 and 0.3) in air

Compound	$NdMnO_3$	$Nd_{0.85}Sr_{0.15}MnO_3$	$Nd_{0.75}Sr_{0.25}MnO_3$	$Nd_{0.7}Sr_{0.3}MnO_3$
σ [S/cm] at 700 °C [31]	25	112(1)	-	200
σ [S/cm] at 800 °C*	-	72.2(1)	131.9(1)	-

*our data

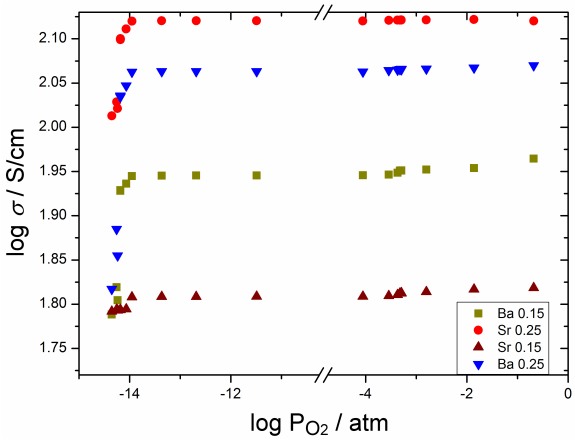

Figure 8. Electrical conductivity isothermal dependences of the of $Nd_{1-x}A_xMnO_{3\pm\delta}$ samples (where x = 0.15 and 0.25 and A = Sr, Ba) on the oxygen partial pressure change in gaseous phase

They show that heating above T = 800 °C and decreasing the oxygen pressure below $P_{O_2} = 10^{-14}$ atm leads to the samples dissociation. The partial oxygen pressure decrease in the range from P_{O_2} of $10^{-14.5}$ to 0.21 atm slightly affects the conductivity of all samples, which indicates its stability under these conditions. However, the decrease of partial pressure P_{O_2} below 10^{-14} atm leads to the sharp decrease of electrical conductivity (Table 3). It confirms our data about beginning of oxide dissociation (Fig. 8). The greatest stability under the experimental conditions is demonstrated by a sample doped with strontium for x = 0.15. Probably the dissociation of this oxide is possible either at prolonged exposure at $P_{O_2} = 10^{-14}$ atm pressure or at lesser oxygen pressure. Thus, an oxygen partial pressure interval has been established at which samples provide stable electrical conductivity at T = 800 °C.

Neodymium replaced by strontium or barium leads to the increased concentration of charge carriers and electrical conductivity:

$$Nd(A)MnO_3 \rightarrow Me'_{Nd} + Mn^{\bullet}_{Mn} + 3\,O^{x}_{O},\ (A = Sr, Ba)$$

The electrical conductivity in air varies from 92.2 (for x = 0.15) to 117.5 S/cm (for x = 0.25) for the Ba-containing samples. Concentration increasing leads to more significant electrical conductivity change (Table 3) if the sample is doped with Sr. This behaviour is explained by higher dopant concentration, which leads to charge carriers number increase in the Mn^{3+}–O_2^-–Mn^{4+} chain.

Electrically conductive perovskites are widely used in a number of different electrical applications if high electrical conductivity at high temperatures is required [31]. For example, they are used as a solid conductor of electrode wire in electric arc welding. Comparison of our data on the electrical conductivity of the studied manganites with the Sheffer *et al.* data [31] shows its good correlation (Table 4). It allows us to recommend $Nd_{1-x}A_xMnO_3$ manganites (where x = 0.15 and 0.25 and A = Sr, Ba) as materials for electric arc welding.

IV. Conclusions

Neodymium replacing by barium or strontium affects the thermal properties of $Nd_{1-x}A_xMnO_3$ oxides (where x = 0.15 and 0.25). The stability of these complex oxides was studied by two methods: static and dynamic. The decrease of partial pressure of oxygen in gas atmosphere determines evolution of phase equilibria in neodymium manganites. Dissociation of the $Nd_{1-x}A_xMnO_3$ (for x = 0,15 and A = Ba, Sr) goes in two stages and begins from oxygen pressure $P_{O_2} = 10^{-14}$ atm. The thermodynamic characteristics of the oxides dissociation reactions and its formation from elements are obtained. Slight increasing of the standard enthalpy and entropy changes of the $Nd_{1-x}A_xMnO_3$ compounds dissociation reactions is observed for x = 0.15 concentration of the Ba or Sr dopant. Besides the entropy of their formation reactions from elements increases are more significant. The opposite trend is observed at dopant concentration of x = 0.25. Stable electrical conductivity of the oxides was found at T = 800 °C and oxygen partial pressures range from air down to $P_{O_2} = 10^{-14}$ atm. It was established that increase of dopant concentration from x = 0.15 to 0.25 leads to the rise of electrical conductivity up to 28% for the samples doped with barium and to 88% for the samples doped with strontium. Thus, the neodymium manganite doped with strontium for x = 0.25 shows the best thermal stability and electrical conductivity.

Acknowledgements: This work had been carried out on the basis of the State Assignment of the Institute

of Metallurgy (Ural Branch of the Russian Academy of Sciences) accoding to the Program of Fundamental Research of State Academies using equipment of the Center for Collective Use Ural-M. The authors are grateful to V. Dimitrov for help in conducted experiments and discussing the results.

References

1. L. Rørmark, S. Stølen, K. Wiik, T. Grande, "Enthalpies of formation of $La_{1-x}A_xMnO_{3\pm\delta}$ (A = Ca and Sr) measured by high-temperature solution calorimetry", *J. Solid State Chem.*, **163** (2002) 186–193.
2. J. Du, T. Zhang, F. Cheng, W. Chu, Z. Wu, J. Chen, "Nonstoichiometric perovskite $CaMnO_{3-\delta}$ for oxygen electrocatalysis with high activity", *Inorg. Chem.*, **53** (2014) 9106–9114.
3. E.V. Tsipis, V.V. Kharton, "Electrode materials and reaction mechanisms in solid oxide fuelcells: A brief review", *J. Solid State Electrochem.*, **12** (2008) 1367–1391.
4. P. Shuk, L. Tichonova, U. Guth, "Materials for electrodes based on rare earth manganites", *Solid State Ionics*, **68** (1994) 177–184.
5. E. Dagotto, T. Hotto, A. Moreo, "Colossal magnetoresistant materials: The key role of phase separation", *Phys. Report*, **344** [1-3] (2001) 1–153.
6. A.K. Kundu, M.M. Selkh, K. Ramesha, C.N.R. Rao, "Novel effect of size disorder on the electronic and magnetic properties of rare earth manganeses of the type $La_{0.7-x}Ln_xBa_{0.3}MnO_3$ (Ln = Pr, Nd, Gd or Dy) with large average radius of the A-site cations", *J. Phys. Condens. Matter.*, **17** (2005) 4171–4180.
7. D.P. Belozorov, A.A. Girich, S.I. Tarapov, A.M. Pogorily, A.I. Tovstolytkin, A.G. Belous, S.A. Solopan, "Left-handed properties of manganite-perovskites $La_{1-x}Sr_xMnO_3$ at various dopant concentrations", *AIP Adv.*, **4** (2014) 037116.
8. Y. Tokura, "Critical features of colossal magnetoresistive manganites", *Rep. Prog. Phys.*, **69** (2006) 797–851.
9. A. Arulraj, R.E. Dinnebier, S. Carlson, M. Hanfland, S. van Smaalen, "Strain effects in perovskite manganites", *Prog. Solid State Chem.*, **35** (2007) 367–377.
10. A.P. Ramirez, "Colossal magnetoresistance", *J. Phys. Condens. Matter.*, **9** (1997) 8171–8199.
11. S.M. Dunaevskii, "Magnetic phase diagrams of manganites in the electron doping region", *Phys. Solid State*, **46** [2] (2004) 193–212.
12. P.G. Radaelli, M. Marezio, H.Y. Hwang, S.W. Cheong, "Structural phase diagram of perovskite $A_{0.7}A'_{0.3}MnO_3$ (A = La, Pr; A′ = Ca, Sr, Ba): A new *Imma* allotype", *J. Solid State Chem.*, **122** [2] (1996) 444–447.
13. S.V. Trukhanov, V.A. Khomchenko, L.S. Lobanovski, M.V. Bushinsky, D.V. Karpinsky, V.V. Fedotova, I.O. Troyanchuk, A.V. Trukhanov, S.G. Stepin, R. Szymczak, C.E. Botez, A. Adair, "Crystal structure and magnetic properties of Ba-ordered manganites $Ln_{0.70}Ba_{0.30}MnO_{3-\delta}$ (Ln = Pr, Nd)", *J. Exper. Theor. Phys.*, **103** [3] (2006) 398–410.
14. I.A. Abdel-Latif, A. Hassen, C. Zybill, M. Abdel-Hafiez, S. Allam, Th. El-Sherbini, "The influence of tilt angle on the CMR in $Sm_{0.6}Sr_{0.4}MnO_3$", *J. Alloys Compd.*, **452** (2008) 245–248.
15. A.I. Kurbakov, A.V. Lazuta, V.A. Ryzhov, "Phase diagram of $Sm_{1-x}Sr_xMnO_3$ perovskite manganites", *J. Phys. Conf. Series*, **200** (2010) 012099.
16. U.Z. Rehman, M.S. Anwar, B.H. Koo, "Influence of barium doping on the magnetic and magnetocaloric properties of $Pr_{1-x}Ba_xMnO_3$", *J. Superconduct. Novel Magn.*, **28** [5] (2015) 1629–1634.
17. E.A. Filonova, A.N. Petrov, "Synthesis, structure, and thermal expansion of $Nd_{1-x}Ba_xMn_{1-y}Cr_yO_3$ solid solutions", *Inorg. Mater.*, **45** [9] (2009)1058–1061.
18. T. Kalmykova, A. Vakula, S. Nedukh, S. Tarapov, A. Belous, V. Krivoruchko, R. Suhov, "Electron spin resonance and magnetic phase transitions in manganite perovskite $La_{0.78}Sr_{0.22}MnO_3$ synthesized by the solid-phase reaction method", *Funct. Mater.*, **25** [2] (2018) 241–245.
19. R.M. Eremina, K.R. Sharipov, L.V. Mingalieva, A.G. Badelin, "Superparamagnetic properties of $La_{1-x}Sr_xMn_{0.925}Zn_{0.075}O_3$ (x = 0.075, 0.095, and 0.115) lanthanum manganites", *JETP Lett.*, **98** (2014) 848–852.
20. M.W. Shaikh, D. Varshney, "Structural and electrical properties of $Pr_{1-x}Sr_xMnO_3$ (x = 0.25, 0.3, 0.35 and 0.4) manganites", *Mater. Sci. Semiconduc. Process.*, **27** (2014) 418–426.
21. M.B. Salamon, M. Jaime, "The physics of manganites: Structure and transport", *Rev. Modern Phys.*, **73** [3] (2001) 583–628.
22. A.M. Yankin, V.F. Balakirev, L.B. Vedmid', O.M. Fedorova, "A static method for studying heterogeneous equilibria", *Russian J. Phys. Chem. A*, **77** [11] (2003) 1899–1902.
23. A.M. Yankin, L.B. Vedmid', "Isobaric prefix to the synchronous thermal analyzer", *RU Patent* 88452, (November 2009).
24. B. Dabrovski, S. Kolesnik, A. Baszczuk, O. Chmaissem, T. Maxwel, J. Mais, "Structural, transport and magnetic properties of $RMnO_3$ perovskites (R = La, Pr, Nd, Sm, ^{153}Eu, Dy)", *J. Solid State Chem.*, **178** (2005) 629–637.
25. O.M. Fedorova, L.B. Vedmid', V.M. Dimitrov, "Effect of oxygen pressure on the thermodynamic stability of $Nd_{0.85}Ba_{0.15}MnO_3$", *Inorg. Mater.*, **55** [10] (2019) 1026–1030.
26. R.D. Shannon, "Reviset effective ionic radii and systematic studies of interatomic distances in halides and chalcogenides", *Acta Cryst. A*, **32** [5] (1976) 751–767.
27. T. Atsumi, N. Kamegashira, "Decomposition oxygen partial pressures of $Ln_{1-x}Sr_xMnO_3$ (Ln = La, Nd and Dy)", *J. Alloys Compd.*, **257** (1997) 161–167.
28. A.I. Vitvitskiy, "Thermal dissociation of crystalline substances", *Russian J. Appl. Chem.*, **89** [2] (2016) 196–199.
29. L.B. Vedmid', A.M. Yankin, O.M. Fedorova, V.M. Dimitrov, "Phase transformations in the Nd–Mn–O system", *Inorg. Mater.*, **51** [3] (2015) 288–293.
30. K.I. Portnoj, N.I. Timofeeva, *Oxygen Compounds of Rare Earth Elements*, Metallurgy, Moscow 1986.
31. D.B. Sheffer, Sh. Tsao, D.D. Najsli, B.K. Narajanan, "Electrode wire with perovskite coating", *RU Patent* 2499656C2 (December2009).